Dynamics of sensorimotor plasticity during exoskeletal finger augmentation

Authors:
Dominika Radziun,[1]*† Siebe Geurts,[1]† Valeria C. Peviani,[1]‡ Luke E. Miller[1]‡

[1]Donders Institute for Brain, Cognition and Behaviour, Radboud University, Nijmegen, the Netherlands

*Corresponding author. Email: dominika.radziun@donders.ru.nl
†,‡ = These authors contributed equally to this work

Abstract
How does the brain integrate artificial body extensions into its somatosensory representation? While previous research shows that tool use can reshape body representations, little is known about how these representations change in response to wearable augmentations across different phases of interaction. In this study, participants wore a custom-built exoskeletal device that extended their fingers by 10 cm. Using a high-density proprioceptive localization task, we measured somatosensory representations of both the biological and artificial fingers at four time points: before, during (pre- and post-use), and after wear. We found three distinct phases of plasticity: wearing the device led to a contraction in perceived finger length; active use caused both biological and artificial finger representations to expand; and a lasting change in biological finger representation remained after device removal. These results show that wearable augmentations are rapidly integrated into somatosensory body maps, with dynamic adjustments shaped by both the structure and use of the device.

Teaser
How do wearable augmentations reshape our sense of the body? Using a custom-built exoskeleton that extended the fingers, we tracked changes in body representations across four stages of wear and use. We found that the sensorimotor system rapidly integrates artificial extensions into its somatosensory map: first contracting, then expanding perceived finger length in response to structure and function, with the shifts persisting after device removal. Our findings reveal dynamic, use-dependent plasticity in body representations, which has direct relevance for designing prosthetics, exoskeletons, and assistive devices.

Introduction

The human body is remarkably adaptable, capable of integrating artificial enhancements that extend its physical capabilities (*1*). This includes traditional tools (e.g., rakes) that operate outside the body as well as body augmentations (e.g., robotic limbs) that directly interface with the user. Decades of research has found that these technologies influence the user's body representations and its implementation in the brain (*1–3*). In contrast, relatively little is known about how body augmentation devices themselves are represented by the user's somatosensory system. Furthermore, most studies use pre-post experimental designs, offering a limited temporal window into the effects of technology. In our study, we aimed to address these gaps by investigating how body augmentation devices are integrated into the body representations over time.

Both tools and augmentation devices drive changes in the user's body representations (*4–11*). Tools alter their user's spatial tactile perception and motor kinematics in ways consistent with stretching the sensorimotor representation of the user's arm (*12–23*). Body augmentation devices, such as extra arms and fingers, are designed to further expand the body's functional capabilities (*24–29*). Controlling an extra robotic finger, the Third Thumb, can modify body representation in sensorimotor cortices (*30*), aligning with evidence that tool use modulates somatosensory processing and induces plasticity in body representations, particularly in secondary somatosensory and posterior parietal cortices (*9*). However, the above effects are almost always measured after the device is no longer in use; how the user's body representation changes once they are directly interfaced with the technology is unclear. Identifying the influence of technological augmentation at other distinct stages—from the initial wearing of the technology to its use and subsequent removal—is crucial for understanding the dynamics of plasticity.

The human nervous system can use proprioceptive feedback to extract the spatial extent of hand-held tools (*11*, *31–35*). This suggests that the sensorimotor system constructs spatial representations of hand-held tools using similar computations as for the body (*36*). It is unknown

whether the same is true of body augmentation technology. Furthermore, it is an open question whether similar spatial plasticity (e.g., stretching) occurs for representations of the technology itself as is it does for body representations (see above).

To characterize the temporal dynamics of plasticity, we developed a novel exoskeletal device that directly interfaced with and extended the user's fingers. Participants completed a proprioceptive localization task (*11*) over four stages: before and after wearing the exoskeleton, and before and after performing motor training tasks that required functional use of the device. This high-density proprioceptive localization task measured how accurately participants could localize different parts of their finger and the exoskeleton in space, allowing us to quantify changes in body representations at different time points.

We observed three time-specific heterogenous effects of the exoskeletal fingers: (i) an initial compression of the user's biological finger representation upon wearing the device, (ii) a stretch of proprioceptive representations of both the user's biological and exoskeletal fingers that was driven by training to use the augmentative device—an effect that was absent after using a non-augmenting device, and (iii) a stretch of the user's finger representation that persisted after the device was removed and was likely driven by persistent exposure to wearing the exoskeleton. Together, these findings offer theoretically important insight into how the brain dynamically integrates artificial extensions into the body representations.

Results

Experiment 1A: Introduction to task protocols and exoskeleton familiarization

The goal of our study was to elucidate the temporal dynamics of somatosensory representational plasticity during body augmentation. To this end, we explored the effects of finger-length augmentation on somatosensory finger representation. Participants (n=18) performed a high-density proprioceptive localization task in which they used their left hand to indicate on a touchscreen where they felt specific target locations on their right index finger, which remained

hidden under the screen. The task involved repeated localization of seven equally spaced points along the length of the finger (and later, also the exoskeleton), enabling fine-grained assessment of perceived spatial structure.

This task was performed at various time points relative to learning to use a finger-extending exoskeleton: before wearing the exoskeleton (stage 1); while wearing the exoskeleton, before using it (stage 2); while wearing the exoskeleton, after using it (stage 3); and after the exoskeleton was removed (stage 4). In all stages, we mapped the participant's representation of their biological index finger. In stages 2 and 3, we also concurrently mapped the participant's exoskeletal finger representation. Statistical tests were evaluated against a Bonferroni-adjusted significance threshold of $\alpha = 0.01$ to account for multiple planned comparisons.

The finger-extending exoskeleton (Fig. 1A) is a 3D-printed structure that elongates the fingers of the user's right hand by 10 cm, mounted on the biological fingertips. Their structure was designed to mimic the biological fingers. It consisted of a central rigid component intended to mimic the bone, surrounded by a padded silicon coating intended to mimic the elasticity of the finger pads and surrounding tissue. The latter ensured greater mechanical compliance during object manipulation, improving the user's success. Crucially, the finger-extending exoskeletal device was designed to explicitly allow us to simultaneously measure spatial perception of both the biological and exoskeletal fingers.

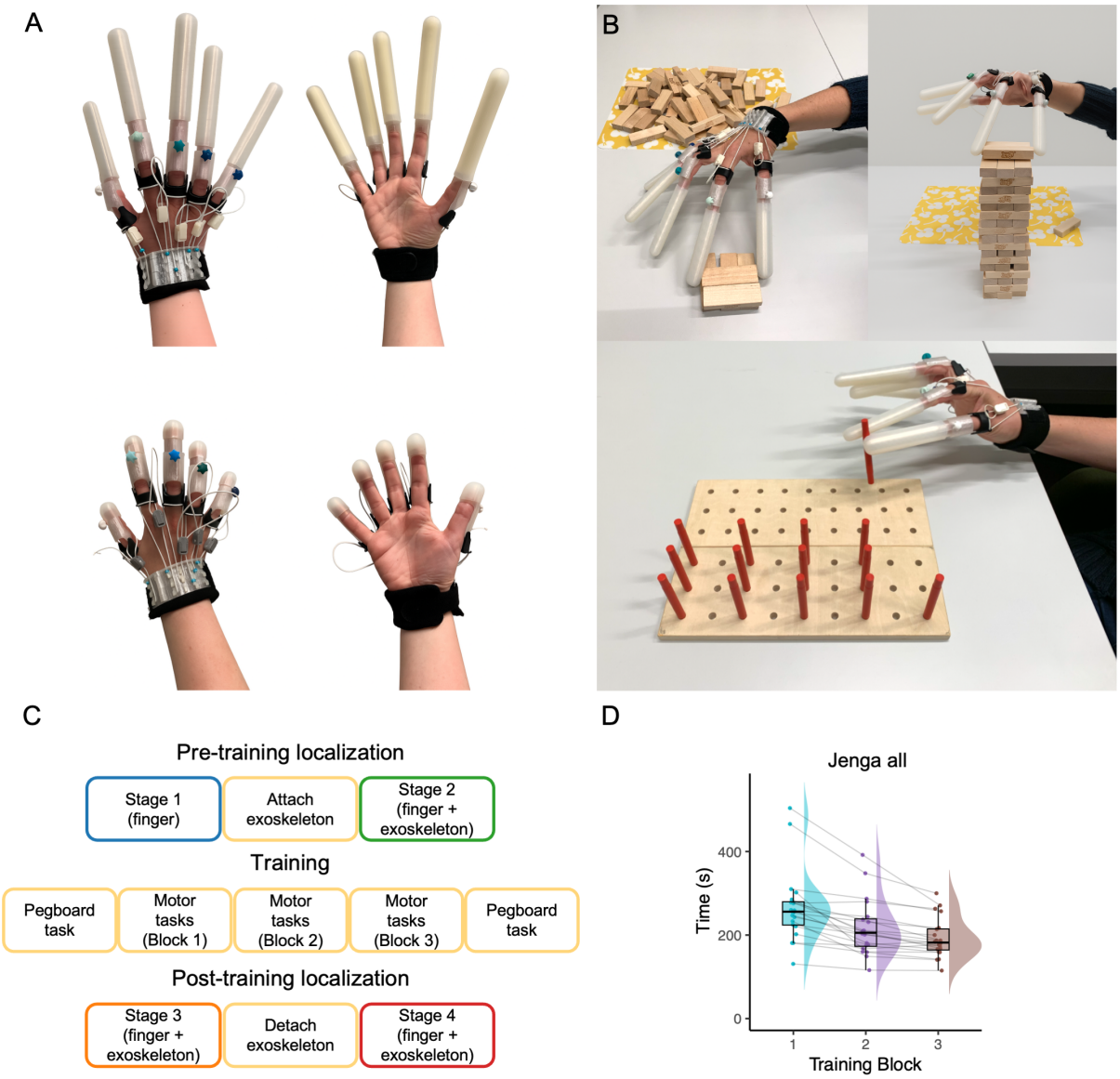

Figure 1. (A) The experimental, finger-extending exoskeleton with 10 cm finger extensions and the control exoskeleton without the extensions. (B) Example of the Jenga stacking training task. Participants wore the exoskeleton and were asked to stack a full Jenga tower; task performance was measured by the time taken to complete the tower. (C) Outline of the experimental design. (D) Group data showing improvement in performance (reduction in completion time) across training blocks.

Wearing the exoskeleton contracts perceived biological finger length

Participants initially localized seven distinct proprioceptive targets on their index finger (stage 1). We then used linear regression to characterize their biological finger representation, modelling their localization judgments as a function of actual target location. This analysis revealed that participants' representation was geometrically accurate, with regression slopes near one (i.e., full accuracy; mean±sem: 1.06±0.09, 95% CI [0.86, 1.25]).

Participants were then fit with the exoskeletal fingers, providing them a short period of visual and proprioceptive feedback about their mechanics and geometry (around 1-2 minutes). They then performed the proprioceptive localization task while wearing the exoskeletons (stage 2). Importantly, the task mapped both the biological and exoskeletal fingers simultaneously (bio+exo).

When wearing the exoskeletal fingers, the combined bio-exoskeleton map was geometrically accurate, spanning the true length of the combined surface (true length: 17.40 cm; estimated length: 18.92 cm; paired *t*-test of map versus true length: $t(17) = -1.25$, $p = .23$, $BF_{10} = 0.48$). How this space was partitioned up, however, was not proportional across surfaces. Specifically, the biological finger segment was significantly under-represented compared to the exoskeletal segment (bio slope mean±sem: 0.85±0.06; exo slope mean±sem: 1.17±0.08; two-tailed paired t-test: $t(17) = -4.37$, $p = .002$, $BF_{10} = 79.66$), only making up 35.25% of the representation (actual: 42.5%). Comparison of the biological finger slopes with the map measured during stage 1 demonstrated that attaching the exoskeletal finger significantly contracted the represented length of the biological finger (19.65% reduction; $t(17) = 2.94$, $p = .046$, $BF_{10} = 5.66$).

Active use of the exoskeleton leads to proprioceptive "stretching" of biological and artificial finger segments

After stage 2, participants completed a 30-45 minute training period to familiarize themselves with the exoskeletal fingers. Training performance improved significantly over time, indicating a clear learning effect and increased proficiency with the device (Fig. 1D). Detailed analyses of individual tasks consistently showed significant improvements across sessions, confirming this effect. Full statistical results and task-specific analyses are provided in the Supplementary Information.

Following training, participants again completed the bio+exo finger localization task (stage 3). Based on previous research with tool use (*12–23*), we hypothesized that training would stretch the user's finger representation. We found that participants' internal mapping of the combined finger (biological + exoskeleton) was no longer geometrically accurate (true length:

17.40 cm; estimated length: 21.18 cm; paired t-test: $t(17) = -3.09$, $p = .007$, $BF_{10} = 7.38$). This served as an initial confirmation of our hypothesis that training with the exoskeleton led to a representational stretch.

We then examined how proprioception of both the biological finger and the artificial exoskeleton segment changed following functional augmentation. The perceived length of the biological finger following training (slope mean±sem: 1.00±0.07, 95% CI [0.86, 1.14]) was significantly longer after training (17.89% increase; $t(17) = 3.67$, $p = .009$ $BF_{10} = 21.65$), demonstrating that finger augmentation stretched the user's finger representation. Interestingly, we identified a similar effect of representational stretch for user's representation of the exoskeletal finger (slope mean±sem: 1.35±0.08, 95% CI [1.19, 1.52]; length change: 15.33% increase; $t(17) = 3.77$, $p = .008$, $BF_{10} = 26.01$). Though stretched, the relative portion of the representation devoted to the finger remained stable (finger proportion 35.22%; paired t-test on proportions before and after training: $t(17) = 0.02$, $p = .96$, $BF_{10} = 4.11$). Together, these findings indicate that proprioceptive representations of both the biological and artificial segments were stretched following training with the finger-extending exoskeleton.

Proprioceptive aftereffects emerge following exoskeleton exposure

After completing the bio+exo localization task (stage 3), participants performed the localization task again with the exoskeleton removed (stage 4). This allowed us to examine whether the representational changes to the biological finger persisted after using the exoskeleton. We did this by comparing the final representation length, measured in stage 4 (slope mean±sem: 1.32±0.08, 95% CI [1.16, 1.49]), with two previous stages: stage 1 and stage 3. Regardless of which set of stages we compared the final mapping to, we observed a similar a modulation in the length of the participant's biological finger representation: an 25.35% increase compared to stage 1 (Fig. 2C; paired t-test: $t(17) = -5.15$, $p < .001$, $BF_{10} = 345.48$); and an increase of 32.33% compared to stage 3 (Fig. 2D; $t(17) = -4.56$, $p = .001$, $BF_{10} = 113.70$).

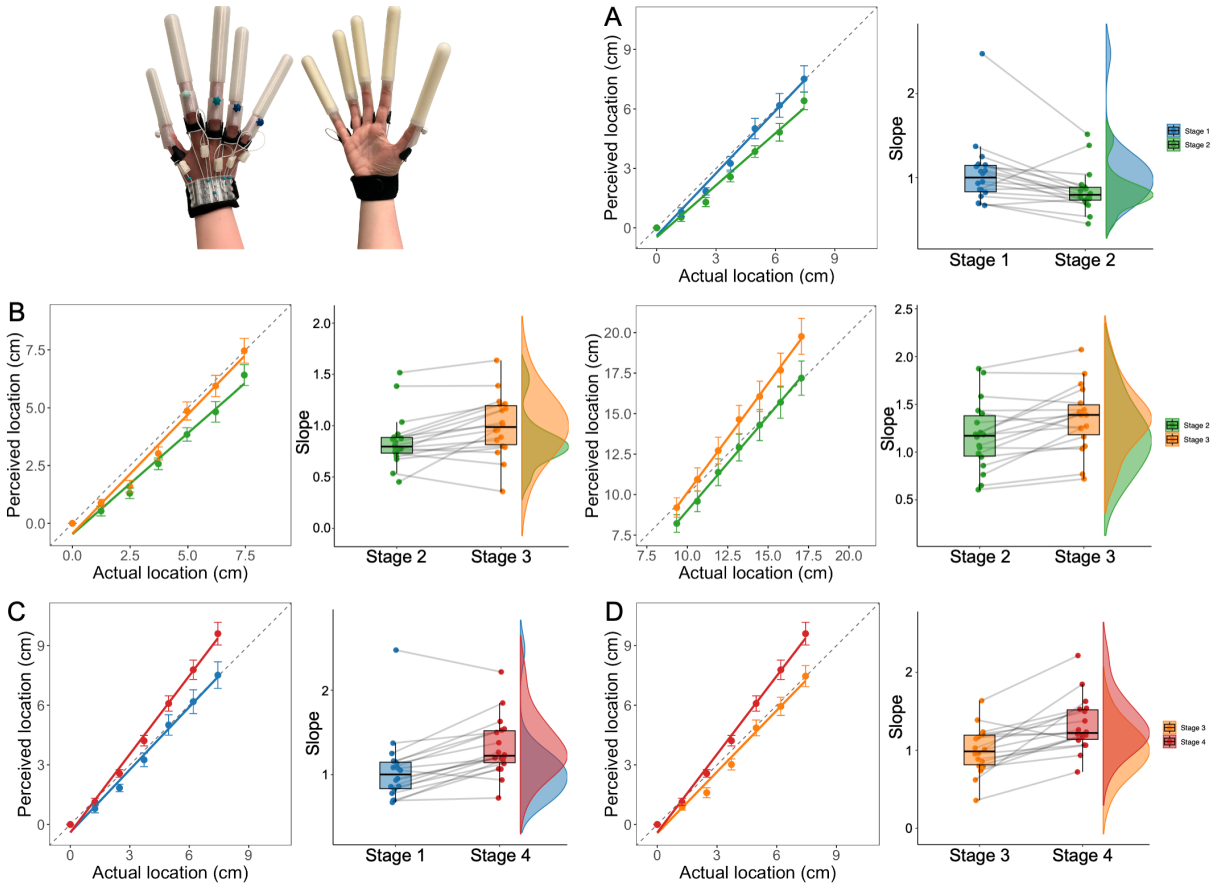

Figure 2. Proprioceptive judgments across stages of augmentation with finger-extending exoskeleton. (A) Comparison of proprioceptive maps from stage 1 (baseline) and stage 2 (initial exoskeleton fitting). (B) Left: Comparison of biological finger segment between stage 2 and stage 3 (after training). Right: Comparison of artificial finger segment between the same stages. (C) Comparison of biological finger representation from stage 1 to stage 4 (post-exoskeleton removal). (D) Comparison of biological finger representation from stage 3 (with exoskeleton) to stage 4 (after removal). In all line plots, perceived location (y-axis) is plotted against actual target location (x-axis). Error bars represent standard error of the mean. The dashed line indicates the identity line (slope = 1). Raincloud plots show individual participant slopes in each stage. The following figure is formatted in the same fashion.

Experiment 1B: A non-augmenting exoskeleton does not stretch the user's proprioceptive representations

We next sought to determine whether the observed training-driven representational stretch (i.e., stage 2 versus 3) was specific to training with an exoskeleton that spatially augmented the user's fingers. To this end, the same eighteen participants took part in the above experimental procedure with one change: the training was done using short exoskeletal fingers that did not meaningfully elongate the fingers (1.4 cm extension; Fig. 1A). Note that all proprioceptive mapping still included the finger-augmenting exoskeleton as in Experiment 1A.

As in Experiment 1A, the combined bio-exoskeleton map obtained during stage 2 (initial localization with the exoskeleton) was overall geometrically accurate (true length: 17.40 cm;

estimated length: 19.38 cm; paired t-test of map versus true length: $t(17) = -1.42$, $p = .17$, $BF_{10} = 0.58$). The biological finger segment was significantly under-represented relative to the exoskeletal segment (bio slope mean±sem: 0.90±0.08; exo slope mean±sem: 1.20±0.09; paired t-test: $t(17) = -3.87$, $p = .006$, $BF_{10} = 31.57$). Furthermore, comparing stage 1 (pre-exoskeleton) to stage 2, we observed that attaching the exoskeletal finger significantly contracted the represented length of the biological finger (19.37% reduction; $t(17) = 4.55$, $p = .001$, $BF_{10} = 112.87$).

We next determined the effect of using the control exoskeleton on the biological and exoskeletal finger representations. Participants were immediately fit with the finger-augmenting exoskeleton after their training with the control exoskeleton. In contrast to Experiment 1A, we did not observe changes in the length of the biological (mean±sem: 0.93±0.07, 95% CI [0.77, 1.09]; $t(17) = -0.69$, $p = 1.00$, $BF_{10} = 0.30$) or exoskeletal finger representation (mean±sem: 1.27±0.09, 95% CI [1.08, 1.45]; $t(17) = -1.68$, $p = .56$, $BF_{10} = 0.78$). This pattern suggests that proprioceptive stretch of somatosensory representations is specific to the active use of the finger-extending exoskeleton, and not simply due to the attachment or observation of them.

Interestingly, we replicated the effect of removing the exoskeletal fingers in stage 4. We observed a similar a modulation in the length of the participant's biological finger representation: a 20.92% increase compared to stage 1 (Fig. 3C; paired t-test: $t(17)= -4.05$, $p = .004$, $BF_{10} = 44.19$); an increase of 44.93% compared to stage 3 (Fig. 3D; paired t-test: $t(17)= -5.42$, $p < .001$, $BF_{10} = 558.70$). Intriguingly, we did not observe a significant difference between the degree of change in Experiment 1A ($t(17) = -0.36$, $p = .72$, $BF_{10} = 0.26$). These results suggest that the proprioceptive aftereffects measured in both experiments was not due to the training stage, but likely to other factors such as wearing the exoskeleton and using proprioceptive feedback of its geometry to perform the localization task.

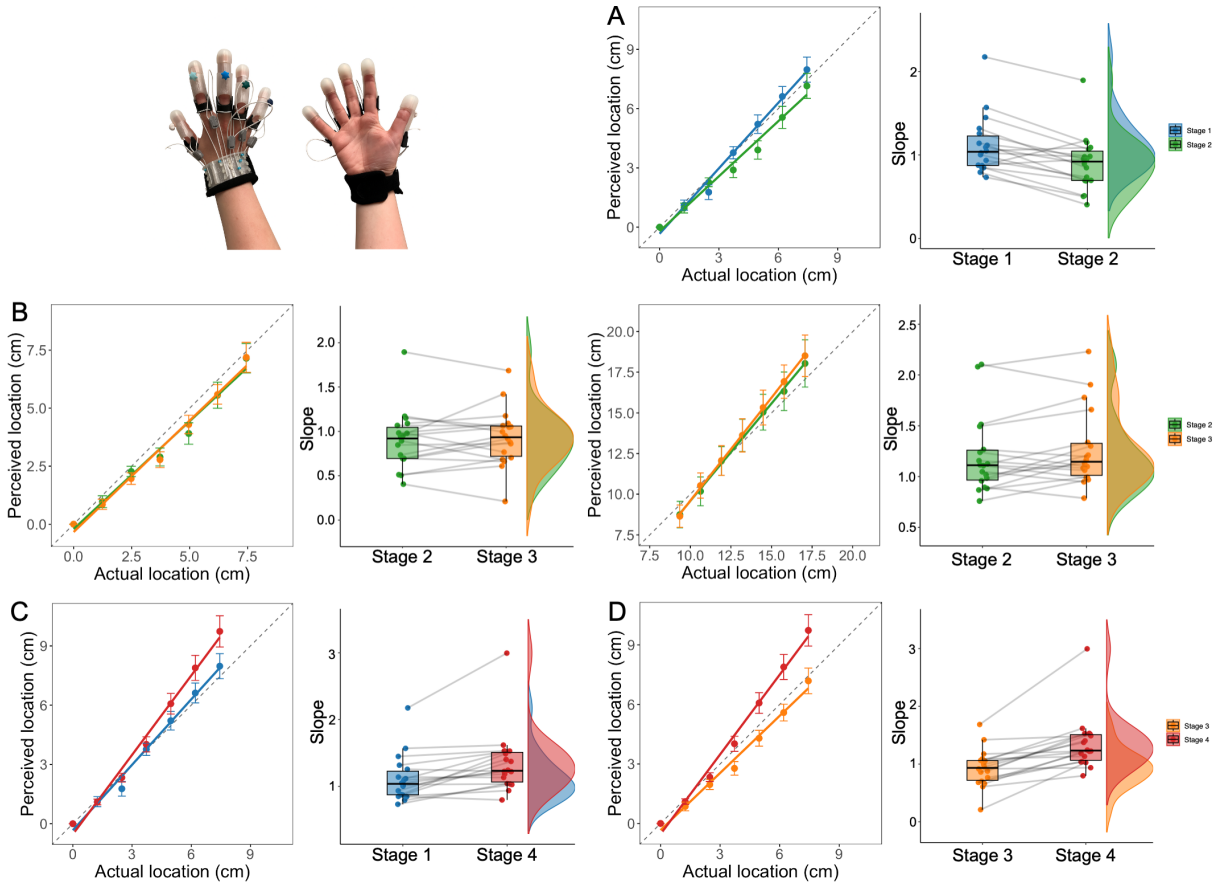

Figure 3. Proprioceptive judgments across stages with training performed using the control device. (A) Comparison of proprioceptive maps from stage 1 (baseline) and stage 2 (initial finger-extending device fitting). (B) Left: Comparison of biological finger segment between stage 2 and stage 3 (after training with control device). Right: Comparison of artificial finger segment between the same stages. (C) Comparison of biological finger representation from stage 1 to stage 4 (post-device removal). (D) Comparison of biological finger representation from stage 3 (after training with control device) to stage 4 (after removal). In all line plots, perceived location (y-axis) is plotted against actual target location (x-axis). Error bars represent standard error of the mean. The dashed line indicates the identity line (slope = 1). Raincloud plots show individual participant slopes in each stage.

Discussion

This study provides a detailed characterization of how the human somatosensory system dynamically adapts to a wearable body-augmenting exoskeleton. Using a high-density proprioceptive localization task, we show that spatial representations of both the biological body and an artificial extension can be flexibly reshaped across time. Specifically, we identified three distinct phases of somatosensory plasticity: an initial contraction of biological finger representation upon wearing the device, a functional "stretching" of both the biological and artificial finger maps following training, and a lasting aftereffect that persisted even after the exoskeleton was removed. Importantly, the emergence of these changes following training demonstrates that humans can

quickly form a somatosensory representation of the exoskeleton based on sensory feedback. While the initial contraction occurred with both the active and control devices, the functional stretching and its associated aftereffects were specific to augmentation with an actively used, finger-extending exoskeleton. Together, our findings reveal how the somatosensory system integrates novel artificial extensions (*2*, *9*).

We show that finger-extending exoskeletons are an effective means for investigating the dynamics of plasticity in body representations. Unlike hand-held tools, exoskeletal devices are directly interfaced with the body (*2*, *3*). Learning to use such a device introduces new demands on proprioceptive processing, requiring the integration of additional structure into the body's representational framework (*37*). Here, we observed that training with the finger-extending exoskeleton led to measurable changes in how both biological and artificial finger segments were represented. These learning-driven changes were absent when participants used a control exoskeleton that did not augment finger length, highlighting the specificity of functional engagement in driving plasticity (*38*, *39*).

The initial act of wearing the exoskeleton, even before use, triggered a reallocation of representational space, leading to a contraction in the represented length of the biological finger (i.e., an under-representation). This suggests that the somatosensory system responds immediately to the presence of an artificial augmentation, even in the absence of task-specific learning. This observation aligns with theories of neural resource allocation, in which new sensory inputs initially compete with existing representations for limited perceptual or cortical resources (*40*). The contraction of the biological finger's representation may reflect an adaptive mechanism, reallocating capacity toward processing novel sensorimotor structures (*9*).

Following training, we observed that both the biological and artificial finger representations underwent a significant stretch, an effect absent when participants trained with the non-extending control device. This parallel plasticity suggests that the brain may apply shared representational

mechanisms to both body parts and technological extensions, reinforcing the idea that augmentation devices can be integrated into the sensorimotor system in a body-like manner (*36*, *41*). The absence of such effect in the control condition emphasizes that this plasticity is not simply a response to attachment, but a specific outcome of using augmentation to achieve new functional outcomes.

One complementary way to viewing our results is via the concept of *internal models*, predictive representations of body dynamics that aid in perception and motor control (*42–44*). Previous work suggests that internal models play a critical role in tool embodiment, allowing the brain to simulate and predict the outcomes of actions involving both the body and its extensions (*33*, *45*). If a user forms biological+technological internal models, then motor learning should modify both similarly. Indeed, we found that the proportion of the overall representation dedicated to the biological and exoskeletal fingers remained constant before and after the observed plasticity. This suggests that the presence of a mechanism that globally stretches the representation of both surfaces, as predicted if the user learned a biological+exoskeleton internal model. This internal model likely underlies the system's ability to coordinate perception and action during interaction with the exoskeleton (*33*, *46*).

This biological+exoskeleton internal model appears to be newly learned during the experiment and is distinct from the user's pre-existing internal model for their fingers. Indeed, we observed a late-stage aftereffect—an increase in biological finger length perception following exoskeleton removal—that occurred both when participants had actively used the finger-extending exoskeleton and when they had only trained with a control device. This suggests that modifying this finger representation did not depend on motor training or functional use of the extension, as was the case with the newly learned internal model. Instead, the pre-existing internal model could be modified with repeated sensory-motor engagement involved in the proprioceptive localization task itself. Importantly, this engagement occurred while participants were still wearing the device,

but its perceptual consequences became apparent only once the exoskeleton was removed and the mapping returned to the biological finger alone.

Despite providing detailed insights into somatosensory plasticity during finger extension via exoskeleton use, our study has limitations that should be considered. The experiments were conducted under short-term, controlled conditions and did not include active sensory feedback from the device, limiting our understanding of how such plasticity unfolds in more ecologically valid or long-term contexts. Moreover, while proprioceptive localization offers a high-resolution behavioral readout of body representation, further research is needed to establish how different forms of sensory feedback, such as tactile or force-based signals, might alter the degree or nature of integration of the body augmentation. Previous studies suggest that even simple visuotactile pairing can support the embodiment of additional digits (*47*), underscoring the potential of multisensory stimulation in shaping body representation. Taken together, these results are especially relevant for the design of next-generation exoskeletons and prosthetics that incorporate artificial sensing to simulate touch. Exploring how the brain integrates these richer feedback channels could help make the artificial extensions to be experienced more like biological body parts rather than external tools. To move toward practical applications, future studies should investigate how neural representations of the finger-extending exoskeletons evolve with extended use and more complex sensorimotor feedback. These directions are essential not only for understanding sensorimotor plasticity, but also for informing the non-invasive restoration of touch in assistive technologies.

In sum, this work demonstrates that the human sensorimotor system is capable of rapidly and flexibly integrating wearable exoskeletons into its spatial framework. Crucially, this integration is shaped by both the physical characteristics of the augmentation and the nature of the user's interaction with it. By showing that proprioceptive representations can quickly adapt to artificial extensions, we provide empirical support for the development of intuitive, body-integrated assistive technologies. Understanding the neural and perceptual mechanisms by which the brain incorporates

such devices has direct implications for neurorehabilitation, prosthetics, and the design of human-machine interfaces that feel like natural extensions of the self.

Materials and Methods

Participants

A total of 20 healthy right-handed participants were recruited (mean age = 27.2 years, range = 18–54; 13 women, 7 men), all of whom completed two experimental sessions on separate days. Two participants were excluded due to the use of undesired strategies to perform the task, resulting in a final sample of 18. One used their visible left hand to mirror the position of their unseen right hand, resulting in atypically high accuracy and low uncertainty. The other switched midway from proprioceptive localization to using a fixed visual reference point, producing a bimodal response distribution. All participants had normal or corrected-to-normal vision and no history of neurological or psychiatric conditions. Participants were asked not to have long nails on the day of the experiment, as this could interfere with the usage of the exoskeleton. The research was approved by the Ethics Committee of the Faculty of Social Sciences, Radboud University. Every participant gave informed consent to participate in the experiment. Participants received a 30-euro voucher or course credits as compensation.

Exoskeletal fingers

The exoskeletal fingers used in this study were custom-built devices designed to augment finger function while interfacing directly with the user's hand. Each device consisted of four finger extensions and a thumb extension, mounted to a wristband. Two exoskeleton sizes, standard and large, were developed to accommodate individual differences in hand size, and an additional medium-width thumb was available for more precise fitting. Of the various size combinations, 10 participants used the small fingers with the small thumb, 8 participants used the small fingers with

the medium thumb, and 2 participants used the large fingers with the medium thumb to ensure a comfortable and functionally effective fit.

The device was constructed from a combination of rigid and flexible materials. The rigid white structural components were 3D printed using PETG filament on Prusa MK3 and MK4 printers. The mechanical joints were printed in PET for greater durability. Molds for casting the outer finger surface were printed in PLA, and the surface itself was made from a skin-safe silicone mixture consisting of Wacker Elastosil Vario 15, Catalyst Vario, and silicone oil.

To cushion the user's fingers, the inner padding was cut from standard paint roller foam and secured inside the fingers using double-sided tape. Tension in the fingers was generated using standard household elastics. Tensioning components were printed in PLA. Stainless steel screws were used throughout the assembly, with nuts press-fit directly into the 3D-printed parts. The colored fingertip components were glued to the screws using superglue, and sharp plastic edges were covered with Pritt Poster Buddies for additional comfort and safety. The wristband was secured using a combination of fine-grain Velcro and standard professional-grade Velcro, sewn together to create a durable and adjustable fastening system.

The final weight of the exoskeleton varied depending on the size and thumb configuration. The standard finger extensions (without thumb) weighed 116 grams, while the large version weighed 134 grams. The thumb components weighed 28 grams (small), 32 grams (medium), and 40 grams (large). Control (non-augmenting) devices were constructed with similar dimensions but were lighter: 60 grams for standard fingers, 67 grams for large fingers, and between 11 and 15 grams for the thumb, depending on size.

Each participant was individually fitted with the appropriately sized exoskeleton. The fitting process consisted of ensuring that the finger caps were as comfortable as possible for the participant and tightening the elastic wires so that the caps were securely attached. After the exoskeleton was

fitted, participants were asked to pick up a small ball to confirm that all components were securely attached and that the device was comfortable to use.

Experimental design

Experiments 1A and 1B used a within-subject control design to isolate the effects of training with the exoskeleton on body representations. The same participants completed both sub-experiments (1A and 1B) on separate days (5–30 days apart), with the order of experiments counterbalanced across participants. Each sub-experiment consisted of three parts: a touchscreen localization task, motor training, and a repetition of the localization task. A final motor task and questionnaire were also included but are not discussed in this article for brevity.

High-density proprioceptive localization task

The participants were seated comfortably in a cushioned chair with their left arm resting on a padded armrest. They were positioned at a table facing the short end of a 93.2 x 52.6 cm LCD touchscreen (iiyama ProLite TF4237MSC-B3AG, Tokyo, Japan), securely fixed above the table. The right arm was placed under the screen on a board with grooves for each finger to ensure consistent placement, and participants were instructed not to look under the screen. The screen displayed three vertical stripes corresponding to the right index, middle, and ring fingers.

Localization task in the four task stages

Stage 1: The task of participants was to localize different locations on their right index finger using proprioception. Throughout the task, the participants kept their right arm completely still and made localization judgments by touching the touchscreen with their left hand (Fig. S1). After the judgment was made, they were asked to move their left hand back to the resting start position, which was 16 cm outside the response field, adjacent to the screen edge.

On a given trial, the procedure was as follows. At the beginning of the trial, an image of a finger was displayed in the lower left corner of the screen. A red dot was placed at the target location within the finger. Participants then pointed on the screen to the corresponding target location on the stripe above their actual index finger. Participants then returned their left hand to the start position. No accuracy feedback was provided. This procedure was repeated for seven equally spaced locations across 20 trials, totaling 140 trials (see Fig. S2A for the layout of target locations). The order was randomized. This task took about 5 to 10 minutes depending on the participant's speed.

Stage 2: The proprioceptive localization task was the same as in stage 1 with the exception that participants now also localized targets within the space of the finger and the finger-augmenting exoskeleton (see Fig. S2B for the layout of the 14 target locations). There were seven distinct target locations within both the biological and exoskeletal finger, for 14 distinct locations in total. There were again 20 trials per location, leading to 280 trials total. This task took around 10 to 15 minutes.

Stage 2 had the distinct procedure that it also required fitting the exoskeletal finger to the participant. After they finished the task in stage 1, they were asked to stay seated and remove their right arm from under the screen. The finger-extending exoskeleton was fitted to their right hand for both experimental and control sessions. After making sure the exoskeleton fit comfortably, the participants' right arm was placed under the screen again in the same position as before.

In Experiment 1A, the participants continued with the finger-extending exoskeleton. In Experiment 1B, after finishing both localization tasks, the finger-extending exoskeleton was removed, and the control exoskeleton was fitted in the same way as the finger-extending exoskeleton.

Stage 3: After completing the motor tasks (see "Training protocol" below), participants were guided back to the touchscreen to repeat the localization task, which was the same proprioceptive localization task as in stage 2. In Experiment 1B, before starting this task, the control exoskeleton was replaced with the finger-extending exoskeleton while the participant was blindfolded. The

blindfold ensured that participants did not see their hand without the exoskeleton, preventing visual input from recalibrating their hand representation and potentially diminishing the effects of the training. In Experiment 1A participants remained wearing the exoskeletal finger.

Stage 4: For the finger-only localization task, the exoskeleton was removed while participants were blindfolded, and their hand was guided back under the screen before the blindfold was removed. Participants then performed the same proprioceptive localization task as in stage 1.

Training protocol

The training took place between stages 2 and 3. During the training, participants were asked to complete a set of tasks to familiarize them with the use of the exoskeletal fingers and train their motor control. They were instructed that the tasks should be completed predominantly with their right, exoskeleton-wearing hand. That is, grasping and manipulation was to be performed solely with the right hand, and they were to only use their left hand in a supportive role when needed, that is, only to stabilize objects or assist minimally without performing the main action. This approach was chosen to make the training more ecologically relevant, as in daily life, both hands would typically be used to complete such tasks. Each task was repeated three times, forming three blocks of trials. Within each block, the order of tasks was consistent for each participant, but this order was randomized across participants.

The tasks included in the training were based on a previously introduced protocol (*30*): building a Jenga tower with wooden blocks, sorting plastic bricks according to their color, and sorting shapes by inserting them into a wooden box. In addition, participants completed the Purdue Pegboard Test (both long and short peg versions) before and after the three repetitions (*48*). See the Supplementary Information for a detailed description of each task.

Data analysis

Linear regression was used to quantify the represented length of finger and exoskeleton. In the localization tasks, the perceived location of each target was calculated as the mean of participants' response distributions. The true position of the targets was determined from participants' finger measurements and the known exoskeleton length. By performing regressions of perceived versus true locations, we obtained an offset (β_0) and a slope (β_1). The offset was discarded, as it only reflected a spatial bias without providing information on length perception. The slope, however, indicates the scaling factor and represents participants' length perception.

For the finger-only localization task, one regression was performed per condition (pre- and post-training), resulting in four slopes per participant (two per sub-experiment). For the finger+exoskeleton localization task, two regressions were performed per condition (pre- and post-training): one for the biological finger segment and one for the exoskeleton segment, yielding eight slopes per participant. These slopes quantified perceived spatial scaling along each segment and served as a measure of perceived length.

The comparison of the represented length involved analyzing the segments separately, leading to two comparisons of condition and pre/post-training. Changes in slope across experimental stages (e.g., before and after training) were evaluated using paired t-tests. We conducted planned comparisons between stage 1 vs. 2 (finger), 2 vs. 3 (finger and exoskeleton), 1 vs. 4 (finger), 3 vs. 4 (finger) within each of Experiment 1A and 1B, resulting in five paired t-tests per experiment. To control for multiple comparisons, we applied a Bonferroni correction within each experiment, setting the adjusted significance threshold at $\alpha = 0.01$. All reported p-values are from two-tailed tests and are accompanied by 95% confidence intervals and Bayes Factors.

References

1. L. E. Miller, A. Farnè, Extending Tactile Space With Handheld Tools: A Re-Analysis and Review. **1**, 1–19 (2024).

2. A. Maravita, A. Iriki, Tools for the body (schema). *Trends Cogn. Sci.* **8**, 79–86 (2004).

3. M. Martel, L. Cardinali, A. C. Roy, A. Farnè, Tool-use: An open window into body representation and its plasticity. *Cogn. Neuropsychol.* **33**, 82–101 (2016).

4. A. Iriki, M. Tanaka, Y. Iwamura, Coding of modified body schema during tool use by macaque postcentral neurones. *Neuroreport* **7**, 2325–2330 (1996).

5. A. Berti, F. Frassinetti, When far becomes near: remapping of space by tool use. *J. Cogn. Neurosci.* **12**, 415–420 (2000).

6. N. P. Holmes, C. Spence, The body schema and the multisensory representation(s) of peripersonal space. *Cogn. Process.* **5**, 94–105 (2004).

7. M. R. Longo, A. Serino, Tool use induces complex and flexible plasticity of human body representations, *The behavioral and brain sciences*. **35** (2012)pp. 229–230.

8. J. P. Gallivan, D. A. McLean, K. F. Valyear, J. C. Culham, Decoding the neural mechanisms of human tool use. *Elife* **2**, e00425 (2013).

9. L. E. Miller, M. R. Longo, A. P. Saygin, Tool use modulates somatosensory cortical processing in humans. *J. Cogn. Neurosci.* **31**, 1782–1795 (2019).

10. J. Eden, M. Bräcklein, J. Ibáñez, D. Y. Barsakcioglu, G. Di Pino, D. Farina, E. Burdet, C. Mehring, Principles of human movement augmentation and the challenges in making it a reality. *Nat. Commun.* **13**, 1345 (2022).

11. V. C. Peviani, L. N. Pfeifer, G. Risso, M. Bassolino, L. E. Miller, Tool use fine-tunes arm and tool maps, *bioRxiv* (2024)p. 2024.06. 06.597694.

12. L. Cardinali, F. Frassinetti, C. Brozzoli, C. Urquizar, A. C. Roy, A. Farnè, Tool-use induces morphological updating of the body schema. *Curr. Biol.* **19**, R478-9 (2009).

13. L. Cardinali, C. Brozzoli, C. Urquizar, R. Salemme, A. C. Roy, A. Farnè, When action is not enough: tool-use reveals tactile-dependent access to Body Schema. *Neuropsychologia* **49**, 3750–3757 (2011).

14. A. Sposito, N. Bolognini, G. Vallar, A. Maravita, Extension of perceived arm length following tool-use: clues to plasticity of body metrics. *Neuropsychologia* **50**, 2187–2194 (2012).

15. E. Canzoneri, S. Ubaldi, V. Rastelli, A. Finisguerra, M. Bassolino, A. Serino, Tool-use reshapes the boundaries of body and peripersonal space representations. *Exp. Brain Res.* **228**, 25–42 (2013).

16. L. E. Miller, M. R. Longo, A. P. Saygin, Tool morphology constrains the effects of tool use on body representations. *J. Exp. Psychol. Hum. Percept. Perform.* **40**, 2143–2153 (2014).

17. F. Garbarini, C. Fossataro, A. Berti, P. Gindri, D. Romano, L. Pia, F. della Gatta, A. Maravita, M. Neppi-Modona, When your arm becomes mine: pathological embodiment of alien limbs using tools modulates own body representation. *Neuropsychologia* **70**, 402–413 (2015).

18. L. E. Miller, A. Cawley-Bennett, M. R. Longo, A. P. Saygin, The recalibration of tactile perception during tool use is body-part specific. *Exp. Brain Res.* **235**, 2917–2926 (2017).

19. V. Bruno, I. Carpinella, M. Rabuffetti, L. De Giuli, C. Sinigaglia, F. Garbarini, M. Ferrarin, How tool-use shapes body metric representation: Evidence from motor training with and without robotic assistance. *Front. Hum. Neurosci.* **13**, 299 (2019).

20. M. Martel, L. Cardinali, G. Bertonati, C. Jouffrais, L. Finos, A. Farnè, A. C. Roy, Somatosensory-guided tool use modifies arm representation for action. *Sci. Rep.* **9**, 5517 (2019).

21. D. Romano, E. Uberti, P. Caggiano, G. Cocchini, A. Maravita, Different tool training induces specific effects on body metric representation. *Exp. Brain Res.* **237**, 493–501 (2019).

22. M. Galigani, N. Castellani, B. Donno, M. Franza, C. Zuber, L. Allet, F. Garbarini, M. Bassolino, Effect of tool-use observation on metric body representation and peripersonal space. *Neuropsychologia* **148**, 107622 (2020).

23. A. J. Najafabadi, D. Küster, F. Putze, B. Godde, Emergence of sense of body ownership but not agency during virtual tool-use training is associated with an altered body schema. *Exp. Brain Res.* **241**, 1721–1738 (2023).

24. I. Hussain, G. Salvietti, G. Spagnoletti, D. Prattichizzo, The soft-SixthFinger: A wearable EMG controlled robotic extra-finger for grasp compensation in chronic stroke patients. *IEEE Robot. Autom. Lett.* **1**, 1000–1006 (2016).

25. L. M. Mooney, H. M. Herr, Biomechanical walking mechanisms underlying the metabolic reduction caused by an autonomous exoskeleton. *J. Neuroeng. Rehabil.* **13**, 4 (2016).

26. C. I. Penaloza, S. Nishio, BMI control of a third arm for multitasking. *Sci. Robot.* **3**, eaat1228 (2018).

27. D. Prattichizzo, M. Pozzi, T. Lisini Baldi, M. Malvezzi, I. Hussain, S. Rossi, G. Salvietti, Human augmentation by wearable supernumerary robotic limbs: review and perspectives. *Prog. Biomed. Eng. (Bristol)* **3**, 042005 (2021).

28. B. Yang, J. Huang, X. Chen, C. Xiong, Y. Hasegawa, Supernumerary robotic limbs: A review and future outlook. *IEEE Trans. Med. Robot. Bionics* **3**, 623–639 (2021).

29. K. Umezawa, Y. Suzuki, G. Ganesh, Y. Miyawaki, Bodily ownership of an independent supernumerary limb: an exploratory study. *Sci. Rep.* **12**, 2339 (2022).

30. P. Kieliba, D. Clode, R. O. Maimon-Mor, T. R. Makin, Robotic hand augmentation drives changes in neural body representation. *Sci Robot* **6** (2021).

31. H. Y. Solomon, M. T. Turvey, Haptically perceiving the distances reachable with hand-held objects. *J. Exp. Psychol. Hum. Percept. Perform.* **14**, 404–427 (1988).

32. N. B. Debats, M. O. Ernst, H. Heuer, Perceptual attraction in tool use: evidence for a reliability-based weighting mechanism. *J. Neurophysiol.* **117**, 1569–1580 (2017).

33. L. E. Miller, L. Montroni, E. Koun, R. Salemme, V. Hayward, A. Farnè, Sensing with tools extends somatosensory processing beyond the body. *Nature* **561**, 239–242 (2018).

34. C. Fabio, R. Salemme, A. Farnè, L. E. Miller, Alpha oscillations reflect similar mapping mechanisms for localizing touch on hands and tools. *iScience* **27**, 109092 (2024).

35. L. Z. Themelis, W. P. Medendorp, L. E. Miller, Gaze-centered spatial coding of touch on a hand-held tool, *bioRxiv* (2025). https://doi.org/10.1101/2025.04.04.647167.

36. L. E. Miller, C. Fabio, F. de Vignemont, A. Roy, W. P. Medendorp, A. Farnè, A somatosensory computation that unifies limbs and tools. *eNeuro* **10**, ENEURO.0095-23.2023 (2023).

37. R. Raisamo, I. Rakkolainen, P. Majaranta, K. Salminen, J. Rantala, A. Farooq, Human augmentation: Past, present and future. *Int. J. Hum. Comput. Stud.* **131**, 131–143 (2019).

38. M. A. Umiltà, L. Escola, I. Intskirveli, F. Grammont, M. Rochat, F. Caruana, A. Jezzini, V. Gallese, G. Rizzolatti, When pliers become fingers in the monkey motor system. *Proc. Natl. Acad. Sci. U. S. A.* **105**, 2209–2213 (2008).

39. M. Biggio, A. Bisio, L. Avanzino, P. Ruggeri, M. Bove, Familiarity with a tool influences peripersonal space and primary motor cortex excitability of muscles involved in haptic contact. *Cereb. Cortex Commun.* **1**, tgaa065 (2020).

40. G. Dominijanni, S. Shokur, G. Salvietti, S. Buehler, E. Palmerini, S. Rossi, F. De Vignemont, A. d'Avella, T. R. Makin, D. Prattichizzo, S. Micera, The neural resource allocation problem when enhancing human bodies with extra robotic limbs. *Nat. Mach. Intell.* **3**, 850–860 (2021).

41. L. E. Miller, C. Fabio, V. Ravenda, S. Bahmad, E. Koun, R. Salemme, J. Luauté, N. Bolognini, V. Hayward, A. Farnè, Somatosensory cortex efficiently processes touch located beyond the body. *Curr. Biol.* **29**, 4276-4283.e5 (2019).

42. D. M. Wolpert, Z. Ghahramani, J. R. Flanagan, Perspectives and problems in motor learning. *Trends Cogn. Sci.* **5**, 487–494 (2001).

43. S. H. Scott, Optimal feedback control and the neural basis of volitional motor control. *Nat. Rev. Neurosci.* **5**, 532–546 (2004).

44. R. Shadmehr, J. W. Krakauer, A computational neuroanatomy for motor control. *Exp. Brain Res.* **185**, 359–381 (2008).

45. K. Kilteni, H. H. Ehrsson, Sensorimotor predictions and tool use: Hand-held tools attenuate self-touch. *Cognition* **165**, 1–9 (2017).

46. H. Imamizu, S. Miyauchi, T. Tamada, Y. Sasaki, R. Takino, B. Pütz, T. Yoshioka, M. Kawato, Human cerebellar activity reflecting an acquired internal model of a new tool. *Nature* **403**, 192–195 (2000).

47. D. Cadete, M. R. Longo, A continuous illusion of having a sixth finger. *Perception* **49**, 807–821 (2020).

48. I. Lawson, Purdue pegboard test. *Occup. Med. (Lond.)* **69**, 376–377 (2019).

Acknowledgments: We would like to thank Sibrecht Bouwstra for her key role in the development of the exoskeletons, as well as the Technical Support Group of the Donders Centre for Cognition for their additional support. **Funding:** This research was supported by an European Research Council Starting Grant (ERC 101076991 SOMATOGPS) and Dutch Research Council VIDI Grant (VI.VIDI.221G.02) to LEM. **Author contributions:** Conceptualization: DR, SG, VCP, LEM; Methodology: DR, SG, VCP, LEM; Investigation: SG; Visualization: DR, SG; Supervision: VCP, LEM; Writing—original draft: DR, LEM; Writing—review & editing: DR, SG, VCP, LEM. **Competing interests:** Authors declare that they have no competing interests. **Data and materials availability:** The data that support the findings of this study will be available from the Open Science Framework upon publication.